ARTICLE

Disruption of an EHMT1-Associated Chromatin-Modification Module Causes Intellectual Disability

Tjitske Kleefstra,[1,2,3,10,*] Jamie M. Kramer,[1,3,4,10] Kornelia Neveling,[1,2,3] Marjolein H. Willemsen,[1,2,3] Tom S. Koemans,[1,3,4] Lisenka E.L.M. Vissers,[1,2,3] Willemijn Wissink-Lindhout,[1] Michaela Fenckova,[1,3,4] Willem M.R. van den Akker,[1,3,4] Nael Nadif Kasri,[3,4,5] Willy M. Nillesen,[1] Trine Prescott,[6] Robin D. Clark,[7] Koenraad Devriendt,[8] Jeroen van Reeuwijk,[1,3] Arjan P.M. de Brouwer,[1,3,4] Christian Gilissen,[1,2,3] Huiqing Zhou,[1,3,9] Han G. Brunner,[1,2,3] Joris A. Veltman,[1,2,3] Annette Schenck,[1,3,4,10,*] and Hans van Bokhoven[1,3,4,10]

Intellectual disability (ID) disorders are genetically and phenotypically highly heterogeneous and present a major challenge in clinical genetics and medicine. Although many genes involved in ID have been identified, the etiology is unknown in most affected individuals. Moreover, the function of most genes associated with ID remains poorly characterized. Evidence is accumulating that the control of gene transcription through epigenetic modification of chromatin structure in neurons has an important role in cognitive processes and in the etiology of ID. However, our understanding of the key molecular players and mechanisms in this process is highly fragmentary. Here, we identify a chromatin-modification module that underlies a recognizable form of ID, the Kleefstra syndrome phenotypic spectrum (KSS). In a cohort of KSS individuals without mutations in *EHMT1* (the only gene known to be disrupted in KSS until now), we identified de novo mutations in four genes, *MBD5*, *MLL3*, *SMARCB1*, and *NR1I3*, all of which encode epigenetic regulators. Using *Drosophila,* we demonstrate that *MBD5*, *MLL3*, and *NR1I3* cooperate with *EHMT1,* whereas SMARCB1 is known to directly interact with MLL3. We propose a highly conserved epigenetic network that underlies cognition in health and disease. This network should allow the design of strategies to treat the growing group of ID pathologies that are caused by epigenetic defects.

Introduction

Intellectual disability (ID) disorders affect about 1%–3% of the western population and are genetically and phenotypically highly heterogeneous. Mutations in more than 400 genes have been identified, yet the genetic cause remains unknown in the majority of individuals with ID.[1] The genetic and phenotypic heterogeneity of ID makes conceptualizing strategies for treatment difficult. However, a number of genes that cause ID appear to act in common molecular and cellular pathways, raising the possibility that a group of genetically heterogeneous individuals with ID could be treated if a common molecular etiology were targeted.[2] One of the emerging mechanisms that appears to be important in ID is the regulation of neuronal function through the epigenetic control of gene transcription.[3] Epigenetic modifications are important factors in the regulation of cognition in animal models, and several well-characterized ID disorders, such as Rett syndrome (MIM 312750), Angelman syndrome (MIM 105830), and Fragile X syndrome (MIM 300624), have a known epigenetic origin.[3,4] Here, we reveal a chromatin-modification module that underlies another group of ID disorders with an epigenetic origin, the Kleefstra syndrome phenotypic spectrum (KSS [see Subjects and Methods]).

The core phenotype of Kleefstra syndrome (MIM 610253) comprises ID, childhood hypotonia, and distinctive facial features.[5–7] KSS can be caused by haploinsufficiency of *EHMT1*, which encodes a histone methyltransferase capable of histone 3 lysine 9 dimethylation (H3K9me2) in euchromatic regions of the genome.[8,9] In our KSS cohort, about 25% of individuals have *EHMT1* loss-of-function mutations.[3] We hypothesized that the "*EHMT1*-negative" individuals have mutations in genes that share a biological function with EHMT1. Here, we report de novo mutations in four functionally related genes in four individuals with KSS, indicating that this subclass of ID is caused by disruption of a common epigenetic module.

Subjects and Methods

Subjects

We have collected a clinically defined cohort of individuals with the core features of Kleefstra syndrome and have identified *EHMT1* loss-of-function mutations in 25% of these individuals.[3] Despite the clinical similarities in our cohort, there is also

[1]Department of Human Genetics, Radboud University Nijmegen Medical Centre, P.O. Box 9101, 6500 HB Nijmegen, The Netherlands; [2]Institute for Genetic and Metabolic Diseases, Radboud University Nijmegen Medical Centre, P.O. Box 9101, 6500 HB Nijmegen, The Netherlands; [3]Nijmegen Centre for Molecular Life Sciences, Radboud University Nijmegen Medical Centre, P.O. Box 9101, 6500 HB Nijmegen, The Netherlands; [4]Donders Institute for Brain, Cognition, and Behaviour, Radboud University Nijmegen Medical Centre, P.O. Box 9104, 6500 HE Nijmegen, The Netherlands; [5]Department of Cognitive Neuroscience, Radboud University Nijmegen Medical Centre, P.O. Box 9101, 6500 HB Nijmegen, The Netherlands; [6]Department of Medical Genetics, Oslo University Hospital, P.O. Box 4950, Nydalen, Oslo N-0424, Norway; [7]Division of Medical Genetics, Department of Pediatrics, Loma Linda University School of Medicine, Loma Linda, CA 92354, USA; [8]Centre for Human Genetics, University of Leuven, P.O. Box 602, 3000 Leuven, Belgium; [9]Department of Molecular Developmental Biology, Faculty of Science, Radboud University Nijmegen
[10]These authors contributed equally to this work
*Correspondence: t.kleefstra@gen.umcn.nl (T.K.), a.schenck@gen.umcn.nl (A.S.)
DOI 10.1016/j.ajhg.2012.05.003.

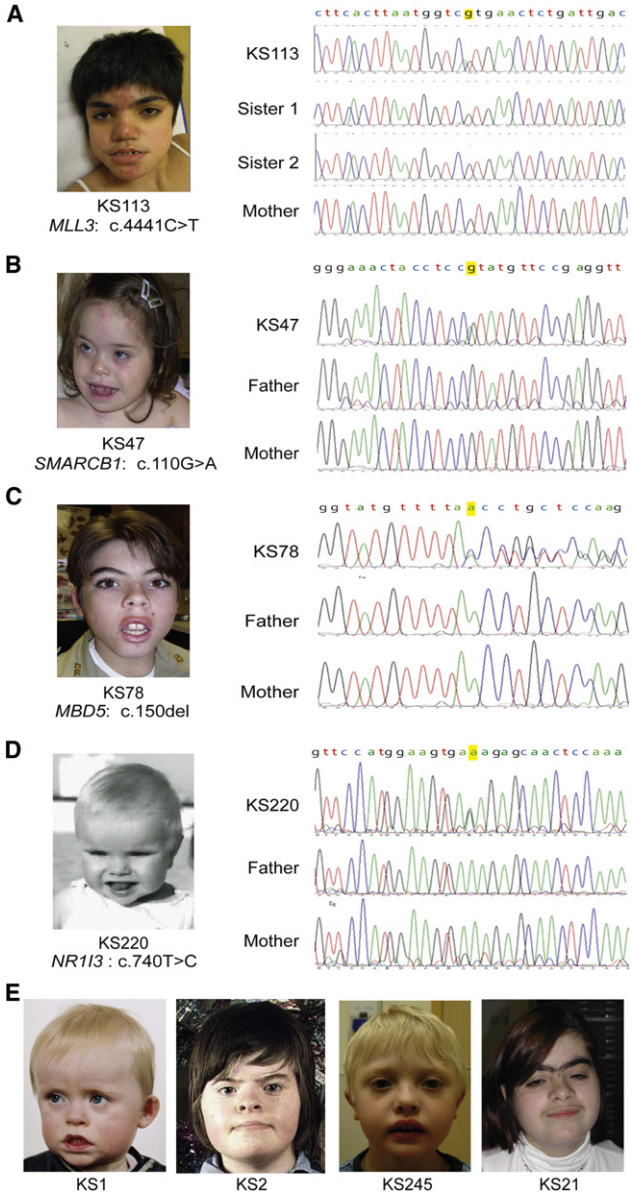

Figure 1. Clinical Photographs and Mutation Information
(A–D) Photographs of individuals with KSS and chromatograms comparing individuals with KSS to parents and/or siblings indicate de novo occurrence for the four probably pathogenic mutations identified. Mutations are highlighted in yellow.
(A) KS113 with *MLL3* mutation c.4441C>T. Reverse-strand sequences of individual KS113, the mother, and two healthy sisters are shown. Note the midface hypoplasia, synophrys, upward slant of palpebral fissures, and everted lower lip.
(B) KS47 with *SMARCB1* mutation c.110G>A, which is not present in the parental DNA. Note the midface hypoplasia, upward slant of the eyes, and tongue protrusion.
(C) KS78 with *MBD5* mutation c.150del, which is not present in the parental DNA. A reverse-strand sequence is shown. Note the synophrys, upward slant of palpebral fissures, upturned nose with broad tip, full lips, and everted lower lip.
(D) KS220 with *NR1I3* mutation c.740T>C, which is not present in the parental DNA. Reverse-strand sequences are shown. Note the midface hypoplasia, short upturned nose, everted lower lip, and pointed chin.
(E) Four KSS individuals (KS1, KS2, KS245, and KS21) with previously published[6,7,10] *EHMT1* defects show a close resemblance of facial characteristics to the four individuals in (A)–(D).

heterogeneity for certain features (e.g., renal anomalies and hearing loss) and significant clinical overlap with other related syndromes, such as Smith-Magenis syndrome (MIM 182290). Therefore, we refer to this group of related phenotypes as KSS. From this study population, we selected nine cases who were found to be negative for *EHMT1* defects and who were previously screened for pathogenic copy-number variants (CNVs) by high-density microarray platforms (Affymetrix 250K microarray equivalent or higher resolution). Informed consent was obtained from all individuals and their parents after approval for the research project was obtained from the institutional ethical board at Radboud University Nijmegen Medical Centre, Commissie Mensgebonden Onderzoek Regio Arnhem-Nijmegen (NL36191.091.11). In this study, we identified de novo mutations in four individuals (Figure 1). General information on medical and developmental characteristics of these four individuals is given below, and their clinical characteristics are compared with those of KSS individuals with *EHMT1* mutations in Table 1.

Individual KS113 was born with a normal birth weight after a normal pregnancy and delivery to nonconsanguineous healthy parents. She walked independently at the age of 19 months but never developed speech. She gradually developed problematic behavior with periods of hyperactivity and aggressiveness. Her total intelligence quotient (TIQ) was 35. At the age of 15 years, she had a height of 148 cm (−2.5 standard deviations [SDs]), a weight of 41 kg (0 SDs), and an occipitofrontal circumference (OFC) of 52 cm (−2 SDs). Additional examinations, including a metabolic screen of blood and urine and DNA analysis of *RAI1*, revealed no abnormalities.

Individual KS47, the second child of healthy nonconsanguineous parents, was born at 36 weeks of gestation after a normal pregnancy with a birth weight of 2,400 g, a length of 49 cm, and head circumference of 33.5 cm. Neonatally, Down syndrome (MIM 190685) was suspected. At the age of 2.5 years, she was shunted for hydrocephalus. At that age, she was not able to sit and did not speak any words. Subsequently, she required multiple neurosurgical procedures for shunt problems because she had an abnormally high production of cerebrospinal fluid as a result of a chorioid plexus anomaly. A partial plexectomy was required, and she has since been clinically stable. She had impaired visual function, which was probably at least partially central in nature. She is myopic (approximately −7 diopters bilaterally). She is a generally sociable person who is interested in her surroundings. At the age of 9.5 years, her height was 144 cm (0 SDs), her weight was 31 kg (−1 SD), and her head circumference was 52.4 cm (0 SDs). No abnormalities were detected on a cardiac ultrasound, a DNA analysis of *UBE3A*, a Southern blot for 15q11-q13, or standard cytogenetic karyotyping in both blood and fibroblasts.

Individual KS78 was born to healthy nonconsanguineous parents. He has three normal siblings, and his 8-month-old brother had laryngomalacia and macrocephaly. Vaginal delivery was induced at 42 weeks of gestation because of a postdate pregnancy. His birth weight was 3,700 g. He had apnea and stridor with laryngomalacia. He walked at 17 months and spoke only single words until after age 3. He was treated with daily growth-hormone injections for one year between the ages of 12 and 13 years, and this treatment resulted in a modest response of about 4 cm. Since then, he has grown only about 1 cm. He had a grand mal seizure between the ages of 2 and 3, but since then, he has had staring spells and mild electroencephalography (EEG) changes. His TIQ was 69 at the age of 12 years. His behavior is characterized by anxiety, a high pain tolerance, stereotypic and self-injurious

Table 1. Clinical Characteristics in Individuals with Different Genetic Causes of KSS

Symptoms	KS113	KS47	KS78	KS220	*EHMT1* Defects
Sex	female	female	male	female	
Intellectual disability	+	+	+	+	100%
Childhood hypotonia	+	+	+	+	100%
Microcephaly	+	−	−	−	20%
Short stature	+	−	+	+	20%
Overweight	−	−	−	−	45%
Brachycephaly	+	+	+	−	40%
Midface hypoplasia	+	+	+	+	80%
Coarse facies	+	+	+	−	50%
Hypertelorism	+	+	+	+	30%
Synophrys	+	+	+	−	60%
Arched eyebrows	−	−	+	−	30%
Short nose	−	+	+	+	45%
Anteverted nostrils	−	+	+	+	25%
Macroglossia (protruding tongue)	−	+	−	+	40%
Tented and cupid-bowed upper lip	+	+	+	+	25%
Thick and everted lower lip	+	−	+	+	25%
Pointed chin	+	−	−	+	25%
Dysplastic ear helices	+	−	−	−	50%
Brachydactyly	−	+	−	−	15%
Cardiac anomaly	−	−	−	−	45%
Renal anomaly	−	−	−	−	15%
Behavioral problems	+	−	+	+	75%
Hearing loss (sensorineural)	−	−	−	−	15%
Seizures	−	−	+	−	25%

behaviors such as hand biting, hand wringing, and spasmodic self-hugging, and bouncing when excited. Several nights a week, he has sleep problems that include 2–3 hr of wakefulness in the middle of the night. He had aggressive outbursts for which he received Abilify (15 mg/day), which reduced the frequency and intensity of the outbursts. At the age of 16 years, he had a short stature (−2 SDs) and macrocephaly (+2 SDs). Additional examinations, including a brain magnetic resonance image (MRI), a metabolic screen of blood and urine, and DNA analysis of *RAI1*, revealed no abnormalities.

Individual KS220 was the third child of healthy, unrelated parents and was born at term after an uneventful pregnancy with a birth weight of 3,300 g, a length of 51 cm, and a head circumference of 36 cm. At the age of 5 months, she developed a pyelonephritis. Her development was severely delayed: At the age of 19 months, her mental development was that of a 12-month-old, and at 4.5 years of age, her development was that of a 2.8-year-old and she attended a special school. Autism spectrum disorder was diagnosed, and she had sleeping difficulties. When she was 5 years and 11 months old, a clinical examination revealed that she had a weight of 15.4 kg (0 SDs), a height of 99 cm (−3.5 SDs), and an OFC of 50 cm (−0.5 SDs). Additional investigations comprising EEG, a brain MRI (at the age 7 of months), and abdominal and cardiac ultrasounds revealed no abnormalities. A screen for metabolic abnormalities and methylation analysis for Angelman and Prader-Willi (MIM 176270) syndromes were normal.

Next-Generation Sequencing

Targeted sequencing was performed on five KSS individuals. The enriched genes were selected from the AmiGO Gene Ontology database (see Web Resources) and comprised all genes annotated with the GO term "chromatin modification" and EHMT1 interactors known from the STRING database (see Web Resources). A total of 316 genes (Table S1, available online) were targeted on a 385K sequence capture array (Roche NimbleGen). The array design comprised all coding exons, including surrounding sequences to cover the splice sites. In total, the design included 4,658 targets comprising 1,429,871 bp. Sequence capture and posthybridization ligation-mediated PCR were done according to the manufacturer's (Roche NimbleGen) instructions with the Titanium optimized protocol. The amplified captured samples were used as input for emulsion PCR (emPCR) amplification and subsequent sequencing with the use of a Roche 454 GS FLX Titanium sequencer. Data analysis was done with Roche Newbler software (v.2.3) and the human genome build hg18 (NCBI Build 36.1). Mapping and coverage statistics were extracted with custom software (Table S2). Sequence variations were automatically detected during mapping, and they were annotated with known RefSeq genes (UCSC hg19, see Web Resources) and SNP information (dbSNP129) with the use of in-house analysis software.[11]

A SOLiD optimized SureSelect Human All Exon Kit (50 Mb, ~21,000 genes; Agilent Technologies) and 3 μg genomic DNA were used for exome sequencing on four trios of parents and their affected children. Library preparation was performed as described previously.[12] To allow for multiplexing, we used posthybridization sample barcodes (Agilent Technologies). Enriched exome libraries were pooled in equimolar sets of four on the basis of a combined library concentration of 0.7 pM. Subsequently, the obtained pool was used for emPCR and bead preparation with the EZbead system (Life Technologies) and for subsequent sequencing with a SOLiD 4 system (Life Technologies). Mapping and variant calling were performed as described previously (Table S3).[13]

For both targeted and exome sequencing, variants and indels were selected with the use of strict quality-control settings, including the presence of at least four (unique) variant reads and at least 15% variant reads. On average, 2,474 and 21,895 variants per proband were annotated for targeted sequencing and exome sequencing, respectively (Table 2).[11,12] For variant prioritization, all nongenic, intronic (other than canonical splice sites), and synonymous variants were excluded, resulting in an average of 94 (targeted) and 5,596 (exome) variants per sample (Table 2). Next, all variants from either dbSNP (dbSNP129 [targeted] or dbSNP132 [exome]) or our in-house database were excluded, reducing the number of variants to an average of 9 (targeted) and 167 (exome) (Table 2). On the basis of the knowledge that KSS is an autosomal-dominant disease caused by de novo mutations, an autosomal-dominant model of inheritance was used for further prioritization, and all inherited variants except for the X-linked changes were excluded. X-linked changes were only

Table 2. Prioritization of Detected Variants in Targeted and Exome NGS

	Targeted NGS					Family-Based Exome Sequencing			
Sample	**KS113**	**KS47**	**KS35**	**KS94**	**KS129**	**Trio KS78**	**Trio KS220**	**Trio KS53**	**Trio KS49**
High-confidence variant calls	2,495	2,452	2,403	2,530	2,488	24,604	19,610	20,858	22,511
After exclusion of nongenic, intronic, and synonymous variants	90	98	81	88	102	6,244	5,182	5,424	5,638
After exclusion of known variants	7	14	7	9	10	158	112	299	98
After exclusion of inherited variants	–	–	–	–	–	4	5	9	3
Confirmed by Sanger sequencing	5	6	3	5	4	1	3	0	0
De novo mutations	1	1	0	0	0	1	3	0	0

The following abbreviation is used: NGS, next-generation sequencing.

excluded when they were present in the paternal DNA. For the trios examined by exome sequencing, inherited variants were excluded by the selection of variants that were only present in the child but not the parents; this resulted in an average number of five potential de novo variants per proband. Of these, one variant, on average, was confirmed to be de novo by Sanger sequencing. For targeted sequencing, the absence of parental next-generation sequencing (NGS) data required validation by Sanger sequencing for all variants. Confirmed variants (Tables S4 and S5**)** were subsequently analyzed in the parental DNA for the determination of the mode of inheritance. On average, five variants were confirmed by Sanger sequencing; of these five, zero to one variant per sample could be proven to be de novo (Table 2).

To further explore the pathogenicity of the de novo variants, we evaluated data from in silico resources. These comprised the genomic evolutionary conservation score (phyloP) as well as PolyPhen-2 and SIFT (see Web Resources), which predict the impact of amino acid substitutions on protein structure and function.

Haplotype Analysis with Short-Tandem-Repeat Markers

Primers to amplify polymorphic short-tandem-repeat markers in 7q36 were designed with the Primer3 program (see Web Resources**)**. An M13 tail was added to the 5′ and 3′ ends of the primers. Markers were amplified with an M13 forward primer labeled with one of the fluorophores—FAM, VIC, NED, or ROX—at the 5′ end and a M13 reverse primer with a 5′-GTTTCTT-3′ added to its 5′ end to reduce tailing. Markers and primer sequences used for haplotype analysis are shown in Table S6. Final PCR products were mixed with eight volumes of formamide and half a volume of Genescan 500 (−250) LIZ Size Standard and were analyzed with the ABI PRISM 3730 DNA analyzer (Applied Biosystems). The results were evaluated by Genemapper (Applied Biosystems).

Genetic Interaction Studies

We performed genetic interaction studies on *Drosophila* by using the UAS/Gal4 ectopic expression system[14] to induce overexpression or RNAi-mediated knockdown[15] of gene orthologs implicated in KSS. Gene orthologs were identified by the reverse BLAST method[16] and analysis of the treefam database.[17] For *MLL3*, *SMARCB1*, and *MBD5*, clear orthologs (*trr*, *snr1*, and *sba*, respectively) were identified. *NR1I3* is formally orthologous to *HR96* because it is monophyletic in phylogenetic analyses.[17] However, it is quite unlikely that the two proteins that they encode are functionally equivalent. HR96 has acquired an internal repeat,[18] which is not seen in NR1I3. This results in a lack of homology in the middle section of the proteins. In contrast, the ecdysone receptor (EcR) is homologous to NR1I3 across the entire length of the protein and has a much higher similarity than does HR96. Protein BLAST of NR1I3 against the *Drosophila* genome gives EcR as the top hit in *Drosophila melanogaster*. We therefore conclude, on the basis of domain composition and amino acid similarity, that *EcR* is the best candidate to be used for functional studies.

Fly stocks were obtained from the Bloomington *Drosophila* Stock Center (Indiana University) and the Vienna *Drosophila* RNAi Center (Institute for Molecular Pathology).[15] For a complete list of publically available stocks that were used, see Table S7. UAS-EHMT flies were described previously.[19] For genetic interaction studies, females of the genotypes *MS1096-Gal4* and *MS1096-Gal4/FM7*d*; UAS-EHMT* were crossed to fly stocks indicated in Table S7. Wing phenotypes were examined in female progeny.

Results

Identification of De Novo Mutations in Epigenetic Regulators in Four Individuals with KSS

To identify mutations in our *EHMT1*-negative cohort of individuals with KSS (Table 1, Subjects and Methods), we used two strategies. Five individuals were analyzed by a targeted approach in which genes involved in chromatin modification were sequenced. Because the targeted approach could limit the possibility of mutation discovery, four other individuals and their healthy parents were analyzed by whole-exome sequencing. The retrieved variants were filtered as described previously so that potential disease-causing mutations could be identified.[12] All variants remaining after filtering were analyzed by Sanger sequencing, which revealed six de novo mutations in four individuals (Tables S4 and S5). Of these six mutations, none were observed in our in-house exome-sequencing database (450 individuals). One, identified in *POF1B* on the X chromosome, was found once in the 8,760 alleles reported in the National Heart, Lung, and Blood Institute (NHLBI) database (Web Resources), which contains data from more than 5,300 exomes (>10,600 alleles), leaving five unique de novo changes identified in this study (Table 3).

Table 3. List of Unique De novo Variants[a] Identified by NGS

Gene	Individual	Sex	RefSeq Accession Number	cDNA Change	Protein Change	PhyloP Score	PolyPhen-2 Prediction	SIFT Prediction	Protein Function
MLL3	KS113	female	NM_170606.2	c.4441C>T	p.Arg1481*	6.2	damaging	deleterious	trimethylates histone H3 at lysine 4 (H3K4me3); central component of the ASC-2 complex
SMARCB1	KS47	female	NM_003073.3	c.110G>A	p.Arg37His	6.88	probably damaging	deleterious	member of the SWI/SNF family of ATP-dependent chromatin-remodeling complexes
MBD5	KS78	male	NM_018328.4	c.150del	p.Thr52Hisfs*31	3.64	–	deleterious	contains a methyl-binding domain that is required for localization to chromatin
MTMR9	KS220	female	NM_015458.3	c.310T>G	p.Ser104Ala	2.09	benign	tolerated	myotubularin-related protein that is atypical because it has no dual-specificity phosphatase domain
NR1I3	KS220	female	NM_001077482.2	c.740T>C	p.Phe247Ser	3.61	probably damaging	deleterious	nuclear hormone receptor that affects chromatin structure through recruitment of chromatin-modifying complexes

The following abbreviations are used: NGS, next-generation sequencing; and SWI/SNF, switch/sucrose nonfermentable.
[a]Nucleotide positions of variants are based on GRCh37/hg19.

Targeted NGS of individual KS113 revealed a nonsense mutation (c.4441 C>T [p.Arg1481*]) in the myeloid/lymphoid or mixed-lineage leukemia 3 gene *MLL3* (NM_170606.2) (Figure 1A, Table 3, and Figure S1A). The father of individual KS113 was deceased, but we could confirm the absence of this mutation in the mother and two healthy sisters, who each carried the same paternal haplotype at the *MLL3* locus as KS113 (Figure S2). This suggests that the mutation occurred as a de novo event.

A single *SMARCB1* missense mutation (c.110G>A [p.Arg37His]; NM_003073.3), predicted to be deleterious, was detected by targeted NGS in individual KS47 and was absent in both parents (Figure 1B, Table 3, and Figure S1B). Interestingly, mutations in this gene as well as in several other genes that encode proteins of the SWI/SNF complex were recently reported to cause Coffin Siris syndrome (CSS [MIM 135900]).[20,21] The core phenotype of CSS is characterized by ID, coarse facial features, microcephaly, and a hypoplastic nail of the fifth finger and/or toe, but the phenotype is also heterogeneous. Germline mutations in *SMARCB1* have also been reported to predispose to familial schwannomatosis (MIM 162091) and meningiomas (MIM 607174), but not to ID.[22–24] However, these tumor-associated mutations are typically loss-of-function alleles, and complete loss of *SMARCB1* expression is seen in tumors after inactivation of the second allele.[25] In contrast, fibroblasts from individual KS47 equally expressed wild-type and mutant alleles (Figure S3), suggesting that substitution of the highly conserved arginine by histidine in individual KS47 might cause altered protein function rather than loss of function. The *SMARCB1* mutations identified in CSS are either missense or in-frame deletions, which suggests that the CSS phenotype might also result from altered protein function.[20] However, the CSS-causing mutations are located at the C-terminus of the protein in, or very near, the conserved SNF5 domain, whereas the mutation that we identified is close to the N-terminus of the protein and is not located in or near a conserved domain. The different locations of these mutations within SMARCB1 might explain the differences in phenotype; however, more mutations will need to be identified before a true genotype-phenotype correlation can be made. All together, these data suggest that, depending on the nature of the mutation, altered SMARCB1 function can lead to diverse forms of ID.

Individual KS78 contains a *MBD5* frameshift mutation (c.150del [p.Thr52Hisfs*31]; NM_018328.4) that results in a premature stop codon (Figure 1C, Table 3, and Figure S1C). Deletions encompassing *MBD5*, as well as intragenic *MBD5* deletions, have previously been identified in cases with a phenotype reminiscent of Smith-Magenis syndrome, which is characterized by ID, facial dysmorphisms, epilepsy, and behavioral problems.[26–28] Individual KS78 with the *MBD5* frameshift mutation shows a striking phenotypic overlap with these individuals, underscoring the previously observed phenotypic similarity between KSS and Smith-Magenis syndrome.[5]

Analysis of individual KS220 (Figure 1D) revealed three de novo mutations (Table S5): a splice mutation (c.1318-1G>C) affecting *POF1B*, a missense mutation (c.310T>G [p.Ser104Ala]; NM_015458.3) affecting *MTMR9*, and a missense mutation (c.740T>C [p.Phe247Ser]) affecting *NR1I3*. The *POF1B* mutation is found in the NHLBI database and is unlikely to cause KSS because homozygous mutations in this gene have been reported to cause premature ovarian failure (MIM 300604) and because

heterozygous carriers have no apparent phenotype.[29] This leaves two unique de novo variants, one in *MTMR9* and one in *NR1I3* (Table 3). The amino acid change p.Ser104Ala caused by the *MTMR9* mutation is considered to be benign by PolyPhen-2 and tolerated by SIFT. Intragenic SNPs in *MTMR9* have been associated with obesity (MIM 606641).[30] The p.Phe247Ser substitution caused by the *NR1I3* (NM_001077482.2) mutation (Figure 1D and Figure S1D) is predicted to have a damaging effect on protein function by both SIFT and PolyPhen-2.

In contrast to their function in neurodevelopment, the biochemical functions of the genes with de novo mutations are well characterized. MLL3 trimethylates histone H3 at lysine 4 (H3K4me3) and is a central component of the activating signal cointegrator-2 (ASC-2) complex ASCOM, which acts as a transcriptional coactivator for nuclear hormone receptors.[31,32] SMARCB1 is a member of the switch/sucrose nonfermentable (SWI/SNF) family of ATP-dependent chromatin-remodeling complexes, which affect transcription by destabilizing histone-DNA interactions and altering nucleosome positions.[33] MBD5 and its paralog MBD6 contain a methyl-binding domain, which is required for their localization to chromatin.[34] MTMR9, encoded by one of two genes with a unique de novo mutation in individual KS220, contains a domain that putatively interacts with SET domains, one of which is present in EHMT1. However, MTMR9 is cytoplasmic, and no functional relationship with chromatin regulators has been reported.[35] The other mutated gene in individual KS220, *NR1I3*, has been extensively studied in liver metabolism, but this gene is also expressed in the brain.[36,37] NR1I3 is a nuclear hormone receptor that affects chromatin structure through recruitment of chromatin-modifying complexes. Given the predicted damaging function of the *NR1I3* DNA variant (in contrast to the benign prediction of the *MTMR9* mutation) and the epigenetic role of the encoded protein, we considered this mutation to be the most likely cause of KSS in individual KS220.

Subsequently, we sequenced *MBD5*, *NR1I3*, and *MLL3* in a cohort of 50 additional individuals with KSS. No pathogenic sequence changes were identified, which most likely reflects the genetic heterogeneity in KSS.

Identification of Functional Connections between *EHMT1*, *MLL3*, *SMARCB1*, *NR1I3*, and *MBD5*

To address the functional relevance of the five identified genes (*MLL3*, *SMARCB1*, *MBD5*, *NR1I3*, and *MTMR9*) with de novo mutations and to further investigate their biological relationship with EHMT1, we conducted genetic interaction studies in *Drosophila*. We carried out our experiments by modulating gene expression in the *Drosophila* wing, a well-established system for genetic interaction studies.[38] Overexpression of *Drosophila EHMT* in the wing consistently causes extra veins in defined regions of the wing (Figures 2A and 2B). We tested whether and how genetic manipulation of *MBD5*, *MLL3*, *SMARCB1*, *NR1I3*, and *MTMR9* homologs (*sba*, *trr*, *snr1*, *EcR*, and *CG5026*, respectively [see Subjects and Methods]) could modulate this EHMT-induced wing phenotype. Expression of *sba/MBD5* alone in the wing induced mild ectopic wing vein formation with about 50% penetrance (Figure 2C). When *sba/MBD5* was overexpressed together with *EHMT*, the EHMT phenotype was strongly enhanced, and this resulted in a consistent disruption of vein patterning and a strong increase in ectopic vein formation (Figure 2D). Thus, EHMT and sba induce similar mild vein phenotypes in the fly wing, and the strongly increased phenotypic severity elicited by their co-overexpression indicates that the two genes genetically interact in a synergistic manner. For the *MLL3* ortholog *trr*, we observed a striking genetic interaction with *EHMT* upon RNA interference (RNAi)-induced knockdown. *Trr* knockdown alone in the fly wing causes a mild phenotype consisting of a mild loss of wing veins and mild upward curvature of the wing (Figure 2E). Combining *trr/MLL3* knockdown with *EHMT* overexpression resulted in fully penetrant pupal lethality resulting from necrosis of the entire developing wing tissue (Figure 2F). This dramatic compound phenotype indicates an antagonistic relationship between trr/MLL3 and EHMT given that knockdown of *trr/MLL3* dramatically enhances the *EHMT* overexpression phenotype. We also attempted to examine interaction of *EHMT* with *snr1/SMARCB1*. However, knockdown of *snr1/SMARCB1* in the wing causes an extremely severe phenotype on its own, which precludes conclusions about potential genetic interactions with *EHMT*. Finally, we investigated genetic interactions with *EcR/NR1I3* and *CG5026/MTMR9*, which both contain de novo missense mutations in individual KS220 (Table 3). Quantification of ectopic wing vein formation (Figure 2G) revealed no effect of *CG5026/MTMR9* knockdown on the *EHMT* overexpression phenotype (Figure 2H), consistent with the notion that the *MTMR9* mutation does not cause KSS. In sharp contrast, the *EHMT* overexpression phenotype was almost completely rescued by heterozygous loss-of-function mutations in *EcR/NR1I3* (Figure 2H), suggesting that EHMT requires EcR/NR1I3 for its activity. Moreover, overexpression of EcR enhanced EHMT-induced ectopic vein formation (Figure 2H), providing strong evidence of a synergistic relationship between EHMT and EcR/NR1I3. These data further suggest that mutations in *NR1I3*, not *MTMR9*, cause KSS.

Discussion

We have identified four genes—*MLL3*, *SMARCB1*, *MBD5*, and *NR1I3*—with de novo mutations in individuals with severe ID and with additional clinical features that closely resemble those caused by *EHMT1* defects. For three of these genes (*MLL3*, *MBD5*, and *NR1I3*), we were able to provide evidence of functional cooperation with *EHMT1* by using genetic interaction experiments in *Drosophila*

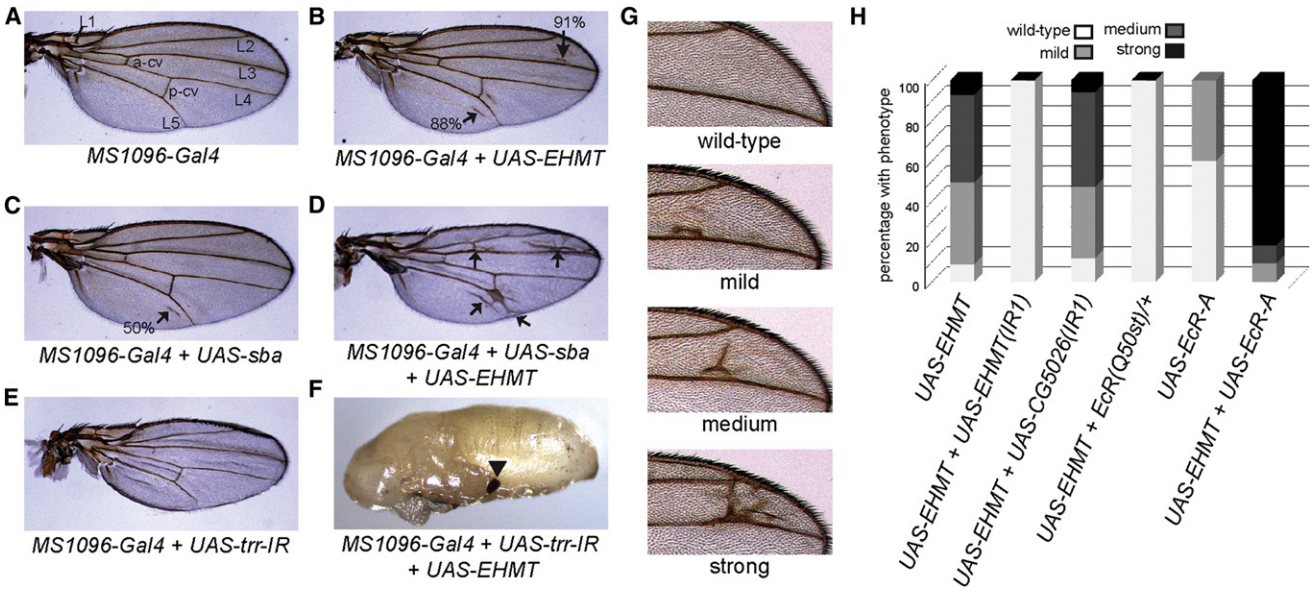

Figure 2. ***Drosophila*** **Orthologs of** ***MBD5, MLL3,*** **and** ***NR1I3*** **Interact Genetically with** ***EHMT***

(A) The morphology of the wild-type *Drosophila* wing is defined by five longitudinal veins (L1–L5) and the anterior and posterior cross veins (a-cv and p-cv).

(B) Tissue-specific overexpression of *UAS-EHMT* in the *Drosophila* wing with the use of *MS1096-Gal4* causes ectopic wing vein formation between L2 and L3 in 91% of wings and between the p-cv and L5 in 88% of wings (arrows).

(C) Expression of *sba*/*MBD5* with *UAS-sba* in the fly wing induced mild ectopic wing vein formation posterior to L5 with about 50% penetrance (arrow).

(D) In combination with *UAS-EHMT*, this phenotype was severely enhanced, resulting in a highly consistent disruption of normal L5 formation and a massive increase in ectopic vein formation between L2 and L3 in all wings examined (arrows).

(E) RNAi-mediated knockdown of *trr*/*MLL3* by induced expression of an inverted repeat (IR) producing double-stranded RNA homologous to *trr* (*UAS-trr*^{IR}) caused mild loss of wing vein L5 and a slight upward curvature of the wing.

(F) In combination with *UAS-EHMT*, *UAS-trr*^{IR} induced pupal lethality caused by the formation of black necrotic tissue in the developing wing (arrowhead). Identical results were obtained with two individual *UAS-trr*^{IR} lines (Table S7). Data is shown for *UAS-trr*^{IR1}.

(G) EHMT-induced ectopic wing vein formation between L2 and L3 is variable in severity and can be quantified accordingly into wild-type, mild, medium, and strong.

(H) The effect of *UAS-EHMT* expression on ectopic vein formation in this region is rescued by RNAi-mediated knockdown of *EHMT* with the use of *UAS-EHMT*^{IR1}. Similar results were obtained with two other *EHMT* RNAi constructs (Table S7). In contrast, *CG5026*/*MTMR9* knockdown had no effect on the EHMT-induced phenotype, as observed with three individual *UAS-CG5026*^{IR} lines (Table S7). Loss-of-function mutations in *EcR* were able to rescue *EHMT*-mediated ectopic vein formation, indicating that *EcR* is required for this *EHMT*-induced phenotype. Similar data were obtained with the *EcR*^{Q50st} allele, the *EcR*^{M554fs} allele, and two *EcR* RNAi lines (Table S7). Overexpression of *EcR* isoform A caused very mild induction of ectopic vein formation. However, in combination with *UAS-EHMT*, *UAS-EcR-A* strongly enhanced *EHMT*-induced ectopic vein formation. Similar results were obtained by overexpression of the other *EcR* isoforms, B1 and B2.

(Figures 2 and 3). However, the severe phenotype of the *SMARCB1*-mutant fly precluded testing for genetic interactions. The established genetic interactions appear to be very specific and thus indicative of a true biological relationship given that a number of other chromatin-related molecules and transcription factors such as *E(z)*, *esc*, *Mier1/CG1620*, and *FoxG/slp2* did not genetically interact with EHMT in our assay (data not shown). Furthermore, no interaction was found with *MTMR9*, one of three de novo mutated genes in individual KSS220. *Drosophila* genetic interaction studies with established disease genes thus provide an efficient and, in our opinion, urgently required method of discriminating between rare or even unique benign DNA variants and causative mutations in the NGS era.

In addition to the genetic interactions established here, complementary evidence of molecular interactions between MLL3/trr, SMARCB1/snr1, and NR1I3/EcR is available. MLL3, a critical subunit of the ASCOM coactivator complex,[28] and SMARCB1, a core component of an ATPase-dependent SWI/SNF chromatin-remodeling complex,[33] are important mediators of epigenetic regulation in association with nuclear-receptor transactivation and directly interact to mediate crosstalk between the two complexes in which they reside.[32,39] NR1I3 was identified as one of the nuclear receptors that directly associates with the ASCOM complex.[39] SMARCB1 and NR1I3 have both been shown to interact with nuclear receptor corepressor 1 (NCOR1).[40,41] In addition, the closest *Drosophila* homolog of NR1I3, EcR, was shown to interact both physically and genetically with the *Drosophila* ortholog of MLL3, trr, indicating that the mechanisms of nuclear-receptor-mediated transcriptional activation are conserved between mammals and flies.[42] These data indicate that

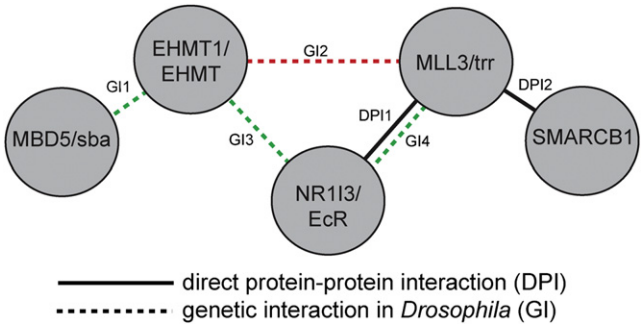

Figure 3. An Epigenetic Network Underlying KSS
Functional studies indicate that genes implicated in KSS occur in a common chromatin-regulating module. This evidence comes from investigation of direct protein-protein interactions (solid lines) and from genetic interaction studies with *Drosophila melanogaster* (dashed lines). Green dashed lines indicate a synergistic interaction, and red dashed lines indicate an antagonistic interaction. It has been demonstrated in this study that *Drosophila EHMT* interacts genetically with *sba*/*MBD5*, *trr*/*MLL3*, and *EcR*/*NR1I3* (GI1, GI2, and GI3, respectively). Previously, genetic and physical interactions between trr and EcR (GI4 and DPI1, respectively), as well as physical association between SMARCB1 and MLL3 (DPI2), have been demonstrated.[32,42]

MLL3, SMARCB1, and NR1I3 cooperate with each other in the regulation of gene transcription (Figure 3).

The molecular and here demonstrated functional relationships between EHMT1 and the other four epigenetic regulators are mirrored by the phenotypic similarities among individuals containing a de novo mutation in any of the five different genes. This leads us to propose a chromatin-modification module, defined by synergistic and antagonistic interactions, that underlies KSS (Figure 3). Further genetic studies in KSS individuals with intact *EHMT1, MLL3*, *SMARCB1*, *MBD5*, and *NR1I3* will most likely reveal additional members of this module. Extension of the KSS chromatin-modification module might also be achieved by the consideration of genes implicated in overlapping phenotypes. This is exemplified in this study through the identification of a mutation in *MBD5*, a gene that is also disrupted in individuals with 2q23.1-deletion syndrome (MIM 156200), which is reminiscent of Smith-Magenis syndrome.[27] Smith-Magenis syndrome and KSS indeed have remarkably overlapping features.[6] Most cases of Smith-Magenis syndrome are caused by haploinsufficiency of *RAI1*, which encodes a transcription factor that acts in conjunction with chromatin-remodeling complexes.[43,44] Finally, other proteins might be added to the module on the basis of established functional relationships despite the fact that mutations in the corresponding genes give rise to disorders with little clinic overlap. This was exemplified in this study through the identification of a missense mutation in *SMARCB1*, which is also mutated in Coffin-Sirus syndrome, another genetically and phenotypically heterogeneous form of syndromic ID. Other examples include the histone demethylase *JARID1C* and the transcriptional regulator *MED12*, which both contain mutations in nonsyndromic ID or ID syndromes without obvious overlapping features.[45,46] However, these epigenetic regulators both have molecular connections to the RE1-silencing transcription factor (REST; also known as NRSF [neuron-restrictive silencer factor]) and to the EHMT1 paralog G9a/EHMT2.[47,48] It is therefore tempting to speculate that a broader spectrum of ID conditions is linked to the core KSS chromatin module.

The identification of a chromatin-modification module underlying ID is of particular interest given recent evidence showing that epigenetic processes are important in acute cognitive functioning.[4] Adult rescue of cognitive deficits has been accomplished in several animal ID models,[42–51] including EHMT-mutant flies,[19] raising hope that cognition can be improved postnatally. Further dissection of the KSS chromatin-regulating module through mechanistic studies and continued elucidation of its genetic etiology might allow for fundamental insights and for the identification of drugs that improve cognition in this group of genetically heterogeneous but phenotypically similar individuals. In this respect, we note that a number of the ID-associated epigenetic regulators, such as MLL3 and SMARCB1, have also been linked to cancer.[23,52] Research into the associated tumorigenic pathways and their applicable drugs might be relevant to neurodevelopmental pathways as well, as was recently shown for topoisomerase inhibitors in a mouse model for Angelman syndrome.[53]

In summary, the work presented here defines and characterizes an epigenetic module underlying human cognitive disorders and underscores the importance of tight epigenetic control mechanisms in higher brain function. In addition, the identification of an EHMT-associated epigenetic module, including antagonistic players that could serve as potential drug targets, is a step toward developing a strategy to correct for cognitive deficits associated with this genetically heterogeneous group of ID disorders.

Supplemental Data

Supplemental Data include three figures and seven tables and can be found with this article online at http://www.cell.com/AJHG.

Acknowledgments

We thank all family members who participated in this study. We would also like to thank the Bloomington *Drosophila* Stock Center and the Vienna *Drosophila* RNAi Center for providing fly stocks. We are grateful to Martijn Huynen for bioinformatics analyses and discussions. This project was supported by the EU FP7 Large-Scale Integrating Project Genetic and Epigenetic Networks in Cognitive Dysfunction (241995 to A.S. and H.v.B.), the EU FP7 project TECHGENE (grant agreement 223143 to J.A.V.), the grant from Hersenstichting Nederland (2009 [1]-122 to T. Kleefstra), the ZonMw (Zorg Onderzoek Nederland) Clinical Fellowship (990700365 to T. Kleefstra), and a Netherlands Organization for Scientific Research Vidi grant (917-96-346) to A.S. Next-generation-sequencing experiments were financially supported by the Department of Human Genetics, Nijmegen.

Received: February 27, 2012
Revised: April 10, 2012
Accepted: May 14, 2012
Published online: June 21, 2012

Web Resources

The URLs for data presented herein are as follows:

AmiGO Gene Ontology database, http://amigo.geneontology.org/cgi-bin/amigo/go.cgi
NHLBI Exome Variant Server, http://snp.gs.washington.edu/EVS/
Online Mendelian Inheritance in Man (OMIM), http://www.omim.org
PolyPhen-2, http://genetics.bwh.harvard.edu/pph2/
Primer3, http://frodo.wi.mit.edu/
SIFT, http://sift.jcvi.org/
STRING database, http://string.embl.de/
UCSC Genome Bioinformatics, http://www.genome.ucsc.edu/

References

1. Ropers, H.H. (2010). Genetics of early onset cognitive impairment. Annu. Rev. Genomics Hum. Genet. *11*, 161–187.
2. van Bokhoven, H. (2011). Genetic and epigenetic networks in intellectual disabilities. Annu. Rev. Genet. *45*, 81–104.
3. van Bokhoven, H., and Kramer, J.M. (2010). Disruption of the epigenetic code: An emerging mechanism in mental retardation. Neurobiol. Dis. *39*, 3–12.
4. Day, J.J., and Sweatt, J.D. (2011). Epigenetic mechanisms in cognition. Neuron *70*, 813–829.
5. Stewart, D.R., and Kleefstra, T. (2007). The chromosome 9q subtelomere deletion syndrome. Am. J. Med. Genet. C. Semin. Med. Genet. *145C*, 383–392.
6. Kleefstra, T., Brunner, H.G., Amiel, J., Oudakker, A.R., Nillesen, W.M., Magee, A., Geneviève, D., Cormier-Daire, V., van Esch, H., Fryns, J.P., et al. (2006). Loss-of-function mutations in euchromatin histone methyl transferase 1 (EHMT1) cause the 9q34 subtelomeric deletion syndrome. Am. J. Hum. Genet. *79*, 370–377.
7. Kleefstra, T., van Zelst-Stams, W.A., Nillesen, W.M., Cormier-Daire, V., Houge, G., Foulds, N., van Dooren, M., Willemsen, M.H., Pfundt, R., Turner, A., et al. (2009). Further clinical and molecular delineation of the 9q subtelomeric deletion syndrome supports a major contribution of EHMT1 haploinsufficiency to the core phenotype. J. Med. Genet. *46*, 598–606.
8. Tachibana, M., Ueda, J., Fukuda, M., Takeda, N., Ohta, T., Iwanari, H., Sakihama, T., Kodama, T., Hamakubo, T., and Shinkai, Y. (2005). Histone methyltransferases G9a and GLP form heteromeric complexes and are both crucial for methylation of euchromatin at H3-K9. Genes Dev. *19*, 815–826.
9. Collins, R.E., Northrop, J.P., Horton, J.R., Lee, D.Y., Zhang, X., Stallcup, M.R., and Cheng, X. (2008). The ankyrin repeats of G9a and GLP histone methyltransferases are mono- and dimethyllysine binding modules. Nat. Struct. Mol. Biol. *15*, 245–250.
10. Willemsen, M.H., Vulto-van Silfhout, A.T., Nillesen, W.M., Wissink-Lindhout, W.M., van Bokhoven, H., Philip, N., Berry-Kravis, E.M., Kini, U., van Ravenswaaij-Arts, C.M., Delle Chiaie, B., et al. (2012). Update on Kleefstra Syndrome. Mol. Syndromol. *2*, 202–212.
11. Hoischen, A., Gilissen, C., Arts, P., Wieskamp, N., van der Vliet, W., Vermeer, S., Steehouwer, M., de Vries, P., Meijer, R., Seiqueros, J., et al. (2010). Massively parallel sequencing of ataxia genes after array-based enrichment. Hum. Mutat. *31*, 494–499.
12. Vissers, L.E., de Ligt, J., Gilissen, C., Janssen, I., Steehouwer, M., de Vries, P., van Lier, B., Arts, P., Wieskamp, N., del Rosario, M., et al. (2010). A de novo paradigm for mental retardation. Nat. Genet. *42*, 1109–1112.
13. Bredrup, C., Saunier, S., Oud, M.M., Fiskerstrand, T., Hoischen, A., Brackman, D., Leh, S.M., Midtbø, M., Filhol, E., Bole-Feysot, C., et al. (2011). Ciliopathies with skeletal anomalies and renal insufficiency due to mutations in the IFT-A gene WDR19. Am. J. Hum. Genet. *89*, 634–643.
14. Brand, A.H., and Perrimon, N. (1993). Targeted gene expression as a means of altering cell fates and generating dominant phenotypes. Development *118*, 401–415.
15. Dietzl, G., Chen, D., Schnorrer, F., Su, K.C., Barinova, Y., Fellner, M., Gasser, B., Kinsey, K., Oppel, S., Scheiblauer, S., et al. (2007). A genome-wide transgenic RNAi library for conditional gene inactivation in Drosophila. Nature *448*, 151–156.
16. Inlow, J.K., and Restifo, L.L. (2004). Molecular and comparative genetics of mental retardation. Genetics *166*, 835–881.
17. Li, H., Coghlan, A., Ruan, J., Coin, L.J., Hériché, J.K., Osmotherly, L., Li, R., Liu, T., Zhang, Z., Bolund, L., et al. (2006). TreeFam: A curated database of phylogenetic trees of animal gene families. Nucleic Acids Res. *34* (Database issue), D572–D580.
18. Schultz, J., Milpetz, F., Bork, P., and Ponting, C.P. (1998). SMART, a simple modular architecture research tool: Identification of signaling domains. Proc. Natl. Acad. Sci. USA *95*, 5857–5864.
19. Kramer, J.M., Kochinke, K., Oortveld, M.A., Marks, H., Kramer, D., de Jong, E.K., Asztalos, Z., Westwood, J.T., Stunnenberg, H.G., Sokolowski, M.B., et al. (2011). Epigenetic regulation of learning and memory by Drosophila EHMT/G9a. PLoS Biol. *9*, e1000569.
20. Tsurusaki, Y., Okamoto, N., Ohashi, H., Kosho, T., Imai, Y., Hibi-Ko, Y., Kaname, T., Naritomi, K., Kawame, H., Wakui, K., et al. (2012). Mutations affecting components of the SWI/SNF complex cause Coffin-Siris syndrome. Nat. Genet. *44*, 376–378.
21. Santen, G.W., Aten, E., Sun, Y., Almomani, R., Gilissen, C., Nielsen, M., Kant, S.G., Snoeck, I.N., Peeters, E.A., Hilhorst-Hofstee, Y., et al. (2012). Mutations in SWI/SNF chromatin remodeling complex gene ARID1B cause Coffin-Siris syndrome. Nat. Genet. *44*, 379–380.
22. Hadfield, K.D., Newman, W.G., Bowers, N.L., Wallace, A., Bolger, C., Colley, A., McCann, E., Trump, D., Prescott, T., and Evans, D.G. (2008). Molecular characterisation of SMARCB1 and NF2 in familial and sporadic schwannomatosis. J. Med. Genet. *45*, 332–339.
23. Christiaans, I., Kenter, S.B., Brink, H.C., van Os, T.A., Baas, F., van den Munckhof, P., Kidd, A.M., and Hulsebos, T.J. (2011). Germline SMARCB1 mutation and somatic NF2 mutations in familial multiple meningiomas. J. Med. Genet. *48*, 93–97.
24. Rousseau, G., Noguchi, T., Bourdon, V., Sobol, H., and Olschwang, S. (2011). SMARCB1/INI1 germline mutations contribute to 10% of sporadic schwannomatosis. BMC Neurol. *11*, 9.
25. Eaton, K.W., Tooke, L.S., Wainwright, L.M., Judkins, A.R., and Biegel, J.A. (2011). Spectrum of SMARCB1/INI1 mutations in familial and sporadic rhabdoid tumors. Pediatr. Blood Cancer *56*, 7–15.

26. Jaillard, S., Dubourg, C., Gérard-Blanluet, M., Delahaye, A., Pasquier, L., Dupont, C., Henry, C., Tabet, A.C., Lucas, J., Aboura, A., et al. (2009). 2q23.1 microdeletion identified by array comparative genomic hybridisation: An emerging phenotype with Angelman-like features? J. Med. Genet. *46*, 847–855.
27. van Bon, B.W., Koolen, D.A., Brueton, L., McMullan, D., Lichtenbelt, K.D., Adès, L.C., Peters, G., Gibson, K., Moloney, S., Novara, F., et al. (2010). The 2q23.1 microdeletion syndrome: Clinical and behavioural phenotype. Eur. J. Hum. Genet. *18*, 163–170.
28. Talkowski, M.E., Mullegama, S.V., Rosenfeld, J.A., van Bon, B.W., Shen, Y., Repnikova, E.A., Gastier-Foster, J., Thrush, D.L., Kathiresan, S., Ruderfer, D.M., et al. (2011). Assessment of 2q23.1 microdeletion syndrome implicates MBD5 as a single causal locus of intellectual disability, epilepsy, and autism spectrum disorder. Am. J. Hum. Genet. *89*, 551–563.
29. Lacombe, A., Lee, H., Zahed, L., Choucair, M., Muller, J.M., Nelson, S.F., Salameh, W., and Vilain, E. (2006). Disruption of POF1B binding to nonmuscle actin filaments is associated with premature ovarian failure. Am. J. Hum. Genet. *79*, 113–119.
30. Yanagiya, T., Tanabe, A., Iida, A., Saito, S., Sekine, A., Takahashi, A., Tsunoda, T., Kamohara, S., Nakata, Y., Kotani, K., et al. (2007). Association of single-nucleotide polymorphisms in MTMR9 gene with obesity. Hum. Mol. Genet. *16*, 3017–3026.
31. Goo, Y.H., Sohn, Y.C., Kim, D.H., Kim, S.W., Kang, M.J., Jung, D.J., Kwak, E., Barlev, N.A., Berger, S.L., Chow, V.T., et al. (2003). Activating signal cointegrator 2 belongs to a novel steady-state complex that contains a subset of trithorax group proteins. Mol. Cell. Biol. *23*, 140–149.
32. Lee, S., Kim, D.H., Goo, Y.H., Lee, Y.C., Lee, S.K., and Lee, J.W. (2009). Crucial roles for interactions between MLL3/4 and INI1 in nuclear receptor transactivation. Mol. Endocrinol. *23*, 610–619.
33. Wilson, B.G., and Roberts, C.W. (2011). SWI/SNF nucleosome remodellers and cancer. Nat. Rev. Cancer *11*, 481–492.
34. Laget, S., Joulie, M., Le Masson, F., Sasai, N., Christians, E., Pradhan, S., Roberts, R.J., and Defossez, P.A. (2010). The human proteins MBD5 and MBD6 associate with heterochromatin but they do not bind methylated DNA. PLoS ONE *5*, e11982.
35. Laporte, J., Bedez, F., Bolino, A., and Mandel, J.L. (2003). Myotubularins, a large disease-associated family of cooperating catalytically active and inactive phosphoinositides phosphatases. Hum. Mol. Genet. *12* (Spec No 2), R285–R292.
36. Nishimura, M., Naito, S., and Yokoi, T. (2004). Tissue-specific mRNA expression profiles of human nuclear receptor subfamilies. Drug Metab. Pharmacokinet. *19*, 135–149.
37. Dutheil, F., Dauchy, S., Diry, M., Sazdovitch, V., Cloarec, O., Mellottée, L., Bièche, I., Ingelman-Sundberg, M., Flinois, J.P., de Waziers, I., et al. (2009). Xenobiotic-metabolizing enzymes and transporters in the normal human brain: Regional and cellular mapping as a basis for putative roles in cerebral function. Drug Metab. Dispos. *37*, 1528–1538.
38. Bier, E. (2005). Drosophila, the golden bug, emerges as a tool for human genetics. Nat. Rev. Genet. *6*, 9–23.
39. Choi, E., Lee, S., Yeom, S.Y., Kim, G.H., Lee, J.W., and Kim, S.W. (2005). Characterization of activating signal cointegrator-2 as a novel transcriptional coactivator of the xenobiotic nuclear receptor constitutive androstane receptor. Mol. Endocrinol. *19*, 1711–1719.
40. Underhill, C., Qutob, M.S., Yee, S.P., and Torchia, J. (2000). A novel nuclear receptor corepressor complex, N-CoR, contains components of the mammalian SWI/SNF complex and the corepressor KAP-1. J. Biol. Chem. *275*, 40463–40470.
41. Jyrkkärinne, J., Mäkinen, J., Gynther, J., Savolainen, H., Poso, A., and Honkakoski, P. (2003). Molecular determinants of steroid inhibition for the mouse constitutive androstane receptor. J. Med. Chem. *46*, 4687–4695.
42. Sedkov, Y., Cho, E., Petruk, S., Cherbas, L., Smith, S.T., Jones, R.S., Cherbas, P., Canaani, E., Jaynes, J.B., and Mazo, A. (2003). Methylation at lysine 4 of histone H3 in ecdysone-dependent development of Drosophila. Nature *426*, 78–83.
43. Bi, W., Saifi, G.M., Shaw, C.J., Walz, K., Fonseca, P., Wilson, M., Potocki, L., and Lupski, J.R. (2004). Mutations of RAI1, a PHD-containing protein, in nondeletion patients with Smith-Magenis syndrome. Hum. Genet. *115*, 515–524.
44. Darvekar, S., Johnsen, S.S., Eriksen, A.B., Johansen, T., and Sjøttem, E. (2012). Identification of two independent nucleosome-binding domains in the transcriptional co-activator SPBP. Biochem. J. *442*, 65–75.
45. Jensen, L.R., Amende, M., Gurok, U., Moser, B., Gimmel, V., Tzschach, A., Janecke, A.R., Tariverdian, G., Chelly, J., Fryns, J.P., et al. (2005). Mutations in the JARID1C gene, which is involved in transcriptional regulation and chromatin remodeling, cause X-linked mental retardation. Am. J. Hum. Genet. *76*, 227–236.
46. Risheg, H., Graham, J.M., Jr., Clark, R.D., Rogers, R.C., Opitz, J.M., Moeschler, J.B., Peiffer, A.P., May, M., Joseph, S.M., Jones, J.R., et al. (2007). A recurrent mutation in MED12 leading to R961W causes Opitz-Kaveggia syndrome. Nat. Genet. *39*, 451–453.
47. Ding, N., Zhou, H., Esteve, P.O., Chin, H.G., Kim, S., Xu, X., Joseph, S.M., Friez, M.J., Schwartz, C.E., Pradhan, S., and Boyer, T.G. (2008). Mediator links epigenetic silencing of neuronal gene expression with x-linked mental retardation. Mol. Cell *31*, 347–359.
48. Tahiliani, M., Mei, P., Fang, R., Leonor, T., Rutenberg, M., Shimizu, F., Li, J., Rao, A., and Shi, Y. (2007). The histone H3K4 demethylase SMCX links REST target genes to X-linked mental retardation. Nature *447*, 601–605.
49. Yan, Q.J., Rammal, M., Tranfaglia, M., and Bauchwitz, R.P. (2005). Suppression of two major Fragile X Syndrome mouse model phenotypes by the mGluR5 antagonist MPEP. Neuropharmacology *49*, 1053–1066.
50. McBride, S.M., Choi, C.H., Wang, Y., Liebelt, D., Braunstein, E., Ferreiro, D., Sehgal, A., Siwicki, K.K., Dockendorff, T.C., Nguyen, H.T., et al. (2005). Pharmacological rescue of synaptic plasticity, courtship behavior, and mushroom body defects in a Drosophila model of fragile X syndrome. Neuron *45*, 753–764.
51. Cobb, S., Guy, J., and Bird, A. (2010). Reversibility of functional deficits in experimental models of Rett syndrome. Biochem. Soc. Trans. *38*, 498–506.
52. Gui, Y., Guo, G., Huang, Y., Hu, X., Tang, A., Gao, S., Wu, R., Chen, C., Li, X., Zhou, L., et al. (2011). Frequent mutations of chromatin remodeling genes in transitional cell carcinoma of the bladder. Nat. Genet. *43*, 875–878.
53. Huang, H.S., Allen, J.A., Mabb, A.M., King, I.F., Miriyala, J., Taylor-Blake, B., Sciaky, N., Dutton, J.W., Jr., Lee, H.M., Chen, X., et al. (2012). Topoisomerase inhibitors unsilence the dormant allele of Ube3a in neurons. Nature *481*, 185–189.